Evidence of Long-T_2 Fraction and Higher Myelin Water Fraction in the Corticospinal Tract

B. A. Russell-Schulz[1], C. Laule[2,3], D. Li[3], and A. L. MacKay[1,3]

[1]Physics and Astronomy, University of British Columbia, Vancouver, BC, Canada, [2]Pathology and Laboratory Medicine, University of British Columbia, Vancouver, BC, Canada, [3]Radiology, University of British Columbia, Vancouver, BC, Canada

Introduction

The corticospinal tract (CST) can be identified on heavily T_2-weighted MR images as areas of bright intensity within the posterior internal capsules [1]. The CST is known to have thicker myelin sheaths than other brain structures [1,2] and this difference in myelin morphology may give rise to a difference in the water T_2 behaviour in the CST. The T_2 decay curve from central nervous system tissue can be separated into several exponential components and in normal brain tissue the T_2 decay curve has three main components, which arise from three distinguishable water environments. There is a shorter component ($T_2 \sim 20$ms), which has been designated as signal from the water trapped within the myelin layers; an intermediate component ($T_2 \sim 80$ms) where the signal arises from intra- and extra- cellular water, and a very long component ($T_2 > 2$s) from cerebrospinal fluid (CSF) [3,4]. These three components can be quantified separately as fractions of the total signal in the area of interest. In addition, a long T_2 component (200ms $< T_2 <$ 800ms) has been observed in the white matter of subjects with PKU and MS, as well as in the CST of normal controls [2,5]. The relationship between myelin content and the amount of long T_2 signal has not been studied in healthy white matter. The purpose of this study is to examine the fraction of long T_2 component and the fraction of myelin water (MWF) in the CST and to compare the results with a nearby structure, the anterior internal capsule (AIC).

Methods

Subjects: Fourteen normal healthy subjects were examined; mean age=27years (range=19-34); 6 males and 8 females.

MR Imaging: Imaging was conducted on a 1.5T Echo Speed GE MR scanner with version 5.7 software. The MR protocol consisted of a localizer, a proton density-weighted and T_2-weighted images (with TR=2500ms and TE=30/80ms) and a modified Carr-Purcell-Meiboom-Gill T_2 relaxation sequence involving 48 echoes to measure the T_2 decay curve. The T_2 sequence used a single 5mm thick axial plane image acquired through the base of the genu/splenium of the corpus callosum (128x128 matrix; first 32 echoes, TE=10ms and TE=50ms for the last 16 echoes, TR=2.12-3.8s with the higher times at low k space values and the lower times at higher k-space values, 4 averages) [6].

Data Analysis: Regions of Interest (ROIs) were drawn bilaterally on the T_2 relaxation experiment around a section of the AIC (TE=10ms, Figure 1A) and the CST (TE=230ms, Figure 1B). The T_2 decay curves were decomposed into a number of exponentials (unspecified apriori) using a non-negative least squares (NNLS) fitting algorithm. The software AnalyzeNNLS was used for analysis [7]. MWF and Long-T_2 fraction (LT2F) maps were created for each subject by displaying the fraction of each component within a voxel where the MWF was the fraction of signal in the T_2 range of 0-40ms and the LT2F was the fraction of signal with T_2 in a range of lower limits 120-145ms to 800ms. The lower limit was selected by observing the LT2F images threshold, which gave rise to signal from the CST but not from the surrounding tissue (See Figure 1C) The MWF and LT2F were determined for each ROI by taking the average fraction from the contributing voxels and bilateral results from each structure were averaged. MWF and LT2F of the AIC and CST were compared using Student's t-test, a p value <0.05 was considered to be significant and the errors presented are standard errors. Regression analysis was also done to investigate the relationship between MWF and LT2F in both the AIC and the CST.

Results

The average MWF for the AIC, 0.057($\pm$0.005), was 66.8% lower than the average MWF for the CST, 0.17($\pm$0.01), (p<10^{-7}). The MWF map for one subject can be seen in Figure 1D. The CST visually shows a higher MWF than the surrounding posterior internal capsule and the AIC. The average LT2F for the AIC, 0.0010($\pm$0.0009) was 99.6% lower than the average LT2F for the CST, 0.22($\pm$0.02), (p<10^{-8}). The LT2F map for one subject can be seen in Figure 1C, The CST shows a distinct brighter intensity at longer T_2 times. Regression analysis revealed that ~50% (R^2=0.4989, p<0.007) of the variance in the LT2F could be accounted for by changes in MWF in the CST (Figure 2), whereas only 1% (R^2=0.0111) of the variance in AIC LT2F could be accounted for by changes in MWF.
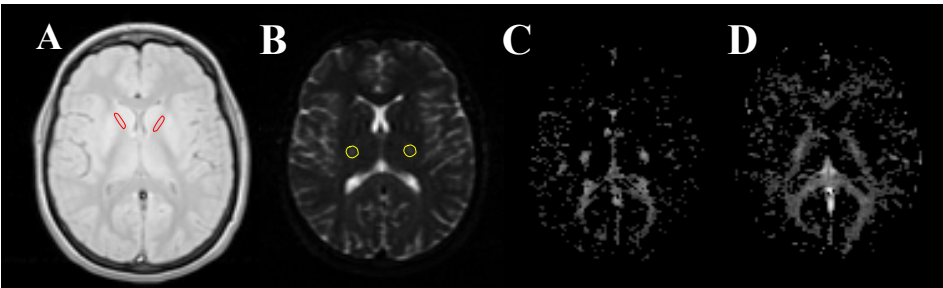

Figure 1: (A) Proton Density weighted image (TE 10ms) (B) T_2-weighted image (TE=230ms) (C) LT2F Map (140ms-800ms) (D) MWF Map (<40ms)
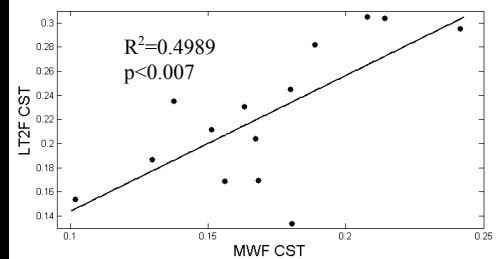
Figure 2: Linear Regression of MWF and LT2F in CST

Discussion/Conclusion

The water reservoir identified here in the CST has a T_2 time greater than 120 ms which is substantially longer than the T_2 time (~ 80ms) typically measured from the intra- and extra- cellular component of central nervous system tissue. The CST also shows a higher MWF than the surrounding tissue (specifically the AIC), which implies an increase in myelin. The CST is known to have thicker myelin sheaths than the surrounding tissue and the results show an increase in the amount of myelin around the CST axons [1]. A previous mammalian brain study estimated the intracellular water content to be 81%$\pm$8%, implying an extracellular water content of about 20% [8] which is close to the LT2F for CST of 22%$\pm$2% measured in this study. This result leads us to speculate that the Long-T_2 signal observed in the cortical spinal tract arises from extracellular water. This signal may not be visible in other brain structures due to exchange between intra- and extra-cellular water in the presence of thinner myelin sheaths. The relationship between MWF and LT2F in the CST will be further investigated in a larger number of subjects and in other structures such as the corpus callosum.

References

1. Yagishita, A., *et al.* Radiology, 191:455-460 (1994)   2. Laule, C., *et al.* JMRI, 26:1117-1121 (2007)   3. Mackay, A., *et al.* Magn Reson Med, 31:673-677 (1994)   4. Whittall, K.P., *et al.* Magn Reson Med, 37:34-43 (1997)   5.Laule, C., *et al.* J Neurol, 254(11):1579-1587 (2007)   6. Sirrs, S.M., *et al.* Neuroradiology, 242(1):236-243 (2007)   7. Bjarnason, T.A., Mitchell, J.R. J Mag Res, 206:200-204 (2010)   8. Quirk, J.D., *et al.* Magn Reson Med, 50:493-499 (2003)